QUANTUM CHEMICAL PREDICTIONS OF ZERO-FIELD NMR SPECTRA OF ORGANIC MOLECULES

Final Report of the CNR-STM project of Dr. **Giacomo Saielli**
"Dipartimento di Scienze Chimiche e Tecnologie dei Materiali"
University of California at Berkeley and Lawrence Berkeley National Laboratory
Berkeley, July 10-31 - 2013

Introduction

I spent three weeks in the research group of Prof. A. Pines (Dept. of Chemistry UCB and Materials Science Division of the Lawrence Berkeley National Laboratory) and in close collaboration with the research group of Prof. D. Budker (Dept. of Physics of UCB and Nuclear Science Division of the Lawrence Berkeley National Laboratory). During my stay I had a chance to visit the NMR laboratory and the instrumentation for the acquisition of Zero-Field NMR spectra (ZFNMR). These spectra result from the modulation of a properly produced magnetization, by the scalar coupling constants *J*. The initial magnetization can be produced by hydrogenation of a double bond by parahydrogen or by an external permanent magnet, though it is not necessary to have high field superconducting magnets. Since the spin system, even for simple molecules, is usually not of first order, the experimental spectra are rather complex and the determination of experimental coupling constants a challenging task.

The purpose of my visit was to simulate ZFNMR spectra by using spin-spin coupling constants calculated by high level quantum chemical methods. This would enable an easier interpretation of the experimental ZFNMR spectra. The theory underlying the ZFNMR spectra has been presented in MC Butler et al. *J. Chem. Phys.* 2013, **138** 184202. ZF is defined as the region where the Zeeman interaction is negligible compared to the scalar couplings occurring in the system, thus in the sub-nT regime. The Earth field (ca. 50 μT) and the magnetic fields produced by all the electronics surrounding the sample need to be "shimmed" down below the desired threshold. The sample needs to be pre-polarised, before the detection in ZF, by i) a relatively strong static field; ii) use of parahydrogen; iii) dynamic nuclear polarization. Subsequent detection, which cannot rely on the high sensitivity of inductive currents, has to be run with a superconductive quantum-interference device or an atomic magnetometer (T. Theis et al. *Nature Phys.* 2011, **7**, 571). Let X and H represent the spin 1/2 heteronucleus (e.g. ^{13}C or ^{15}N) and the proton ^{1}H: for an isolated spin system the ZFNMR spectrum of a simple XH is characterized by a resonance at *J*; for a XH_2 we expect single resonance at 3/2*J*; for a XH_3 system we expect two resonances, one at *J* and another one at 2*J*. Long range couplings to other spins, e.g. protons or other carbons in ^{13}C labeled samples, produce a very complex pattern that cannot be easily understood. Therefore, *first principle* prediction of NMR coupling constants to simulate the ZFNMR spectrum appears as a valid tool for spectral interpretation. The simulation of the ZFNMR spectrum is based on the solution of the eigenvalue problem for a system governed by a Hamiltonian which only contains the spin-spin coupling terms: $\mathbf{H}_J = \Sigma_{jk}\, h/2\pi\, J_{jk}\, \mathbf{I}_j \bullet \mathbf{I}_k$ where $\mathbf{I}_j$ and $\mathbf{I}_k$ are the spin operators of *j* and *k* spins, respectively.

Several systems have been considered during my visit: *i)* pyridine and the isomers of picoline ^{15}N labeled; *ii)* the complex 11-spins system of natural abundance ethylbenzene (six different isotopomers); *ii)* doubly ^{13}C labeled ethylene glycol (EG, $HO^{13}CH_2{}^{13}CH_2OH$) at various temperatures. The results obtained for all these systems will be described in the next Section.

Results

Pyridines The structure of pyridine and of the three isomers of methylpyridine (2-, 3- and 4-methylpyridine) has been minimized at the MP2/aug-cc-pVTZ while NMR calculations were run at the BHandH/pcJ-3 level to predict the whole set of spin-spin coupling constants involving ^{1}H and ^{15}N nuclei. The experimental spectrum of ^{15}N labeled pyridine was obtained after polarization with parahydrogen through the coordination to the Crabtree's catalyst (T Theis et al. *J. Am. Chem. Soc.* 2012, **134**, 3987). This approach is called Non Hydrogenative ParaHydrogen Induced Polarization, NH-PHIP: the polarization brought by parahydrogen is transferred to the pyridine molecule after both are coordinated to the Iridium center of the catalyst. The experimental spectrum is shown in Figure 1 and it features a main resonance around 16

Hz corresponding to 3/2*J* where *J* is the largest coupling in the system, that is $^{2}J(^{15}N,^{1}H)$. Due to the symmetry of pyridine this is an XH_2 system. The spectrum is, however, complicated by several other resonances, notably around 20 Hz, around 13 Hz and at lower frequencies due to the complex network of NH and HH couplings.

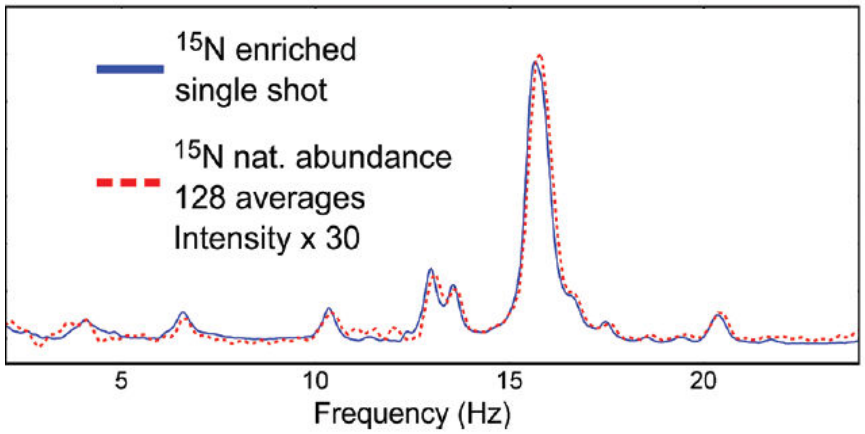

Figure1: Experimental ZFNMR spectra of pyridine obtained by Non-Hydrogenative ParaHydrogen Induced Polarization (NH-PHIP). From T Theis et al. *J. Am. Chem. Soc.* 2012, **134**, 3987.

In table we report the calculated couplings at the BHandH/pcJ-3//MP2/aug-cc-pVTZ level.

Table 1: Calculated spin-spin coupling constants of pyridine, BHandH/pcJ-3//MP2/aug-cc-pVTZ

J(X,Y)	pyridine
$^{2}J(^{15}N,H2)$	−11.85
$^{3}J(^{15}N,H3)=$	−1.32
$^{4}J(^{15}N,H4)$	0.29
$^{3}J(H2,H3)$	5.57
$^{4}J(H2,H4)$	1.60
$^{5}J(H2,H5)$	1.36
$^{4}J(H2,H6)$	−0.66
$^{3}J(H3,H4)$	8.46
$^{4}J(H3,H5)$	1.10

The ZFNMR simulated spectrum is shown in Figure 2 and it nicely reproduces all the main features of the experimental spectrum although all resonances are slightly offset because of a systematic overestimation of the calculated parameters compared to the experimental one.

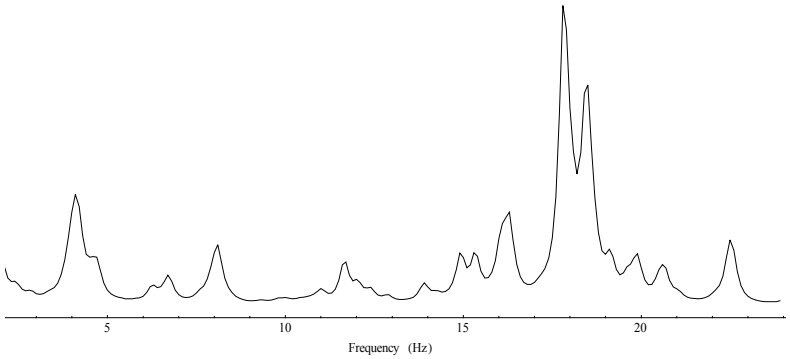

Figure 2: Simulated ZFNMR spectrum of pyridine using the QM calculated NMR spin-spin couplings.

We now turn our attention to the three isomers of methylpyridine. The calculated parameters are reported in Table 2 and the simulated spectra obtained using such spin-spin coupling constants are shown below. The simulated spectra show a remarkably different pattern that would allow an easy assignment of the experimental spectra. These measurements are currently in progress in the Berkeley's groups as part of our on-going cooperation.

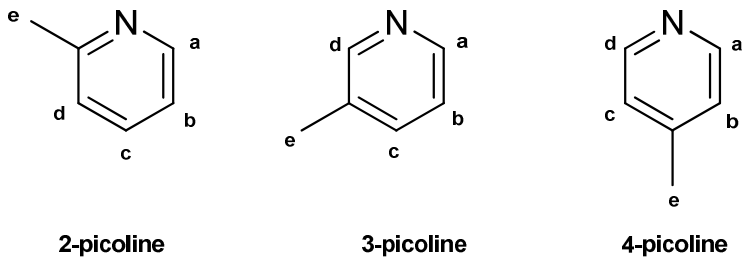

2-picoline **3-picoline** **4-picoline**

Table 2: Calculated coupling constants $J(^{15}N,^{1}H)$ and $J(^{1}H,^{1}H)$ in the three isomers of methylpyridine.

^{n}J(X,Y)	2-picoline	3-picoline	4-picoline
N,H_a	-11.22	-11.21	-11.14
N,H_b	-1.89	-1.88	-1.80
N,H_c	0.76	0.59	-1.80
N,H_d	-1.47	-11.22	-11.14
N,H_e	-3.87	0.76	-0.87
H_a,H_b	6.04	5.96	6.18
H_a,H_c	1.31	1.07	1.31
H_a,H_d	1.38	-0.85	-0.74
H_a,H_e	0.62	-1.07	0.64
H_b,H_c	8.73	8.98	1.48
H_b,H_d	0.72	1.32	1.26
H_b,H_e	-1.01	0.70	-1.16
H_c,H_d	8.86	1.81	6.34
H_c,H_e	0.64	-1.10	-1.03
H_d,H_e	-0.92	-1.19	0.64

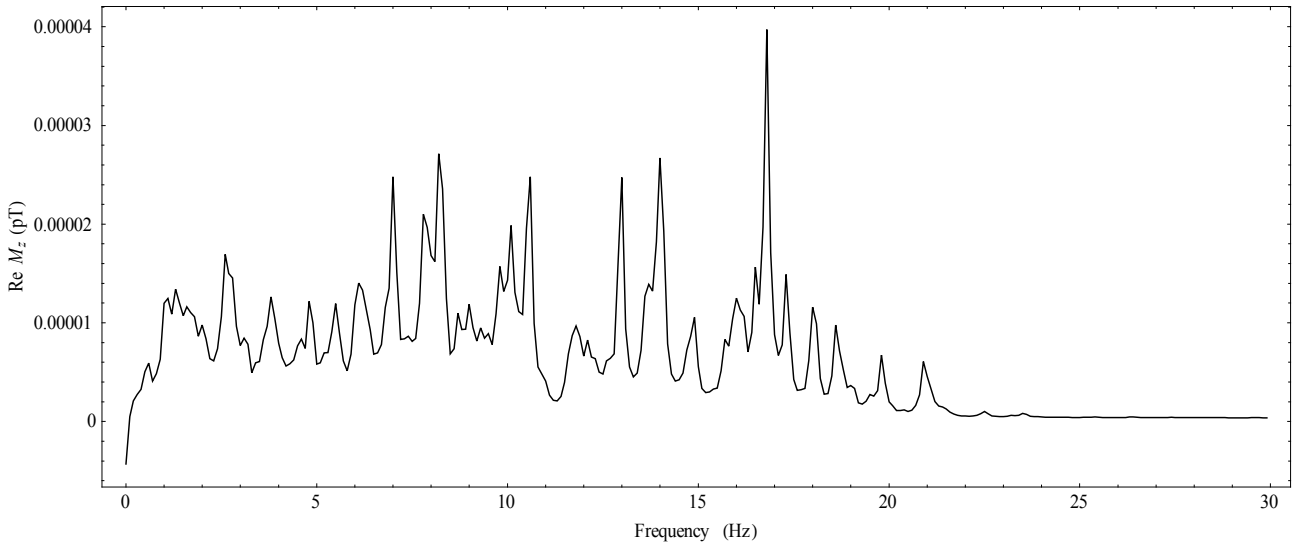

Figure 3: Simulated ZFNMR spectrum of 2-picoline using the QM calculated NMR spin-spin couplings.

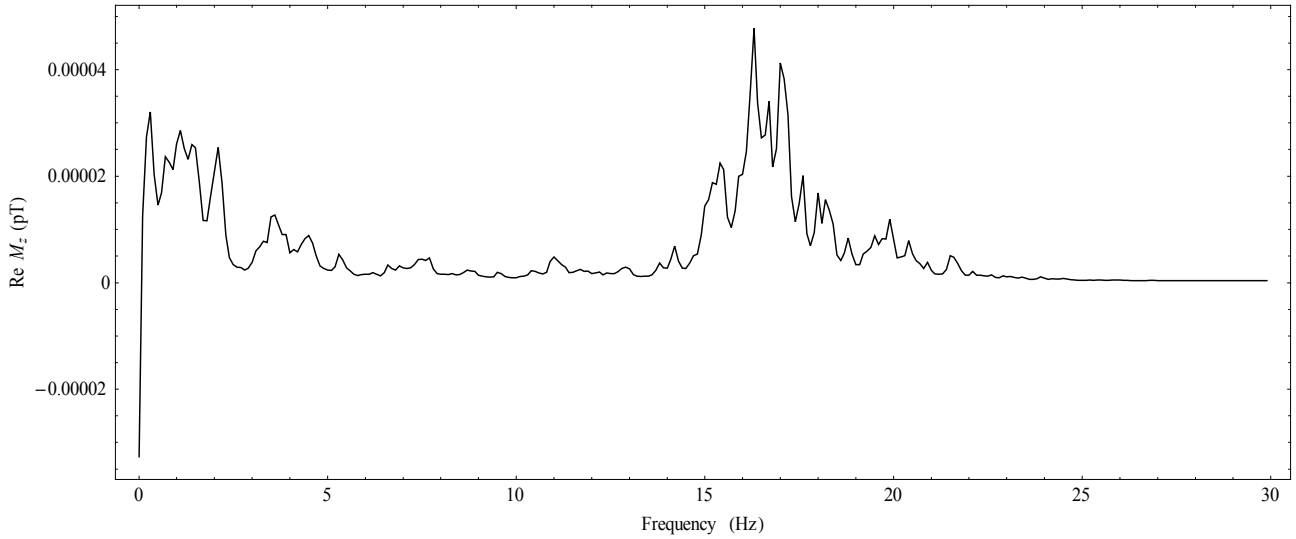

Figure 4: Simulated ZFNMR spectrum of 3-picoline using the QM calculated NMR spin-spin couplings.

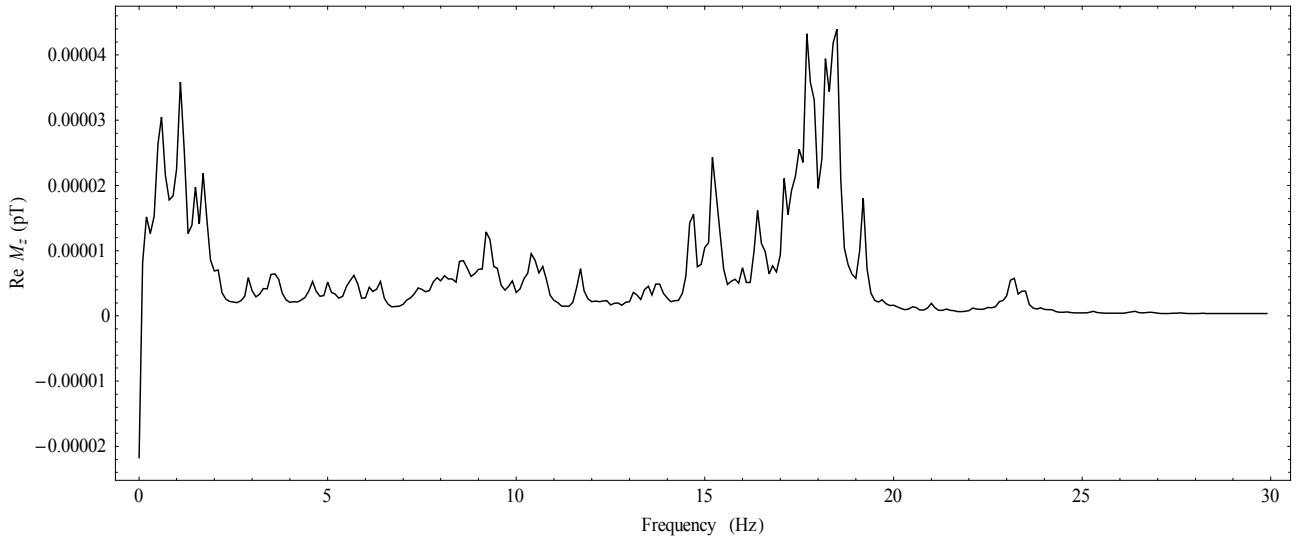

Figure 5: Simulated ZFNMR spectrum of 4-picoline using the QM calculated NMR spin-spin couplings.

The ZFNMR spectrum of 2-picoline appears particularly complex: despite the presence a NH spin system with a relatively larger coupling, compared to the other couplings, there is no evidence of a dominant feature around *J*; instead multiple resonances are observed more or less evenly distributed between 0 and just above 20 Hz. In contrast, 3- and 4-picoline have qualitatively similar spectra where the strong resonance around 3/2*J* due to the $^{15}NH_2$ spin system with the *ortho* hydrogens is observed.

Ethylbenzene. Experimental ZFNMR spectra of ethylbenzene were presented by the Berkeley group (T Theis et al. *Nature Phys.* 2011, **7**, 571).
The experimental spectrum is obtained in natural ^{13}C abundance, after the sample is polarized by addition of parahydrogen to styrene. It is, therefore, the overlap of six different spectra due to the six different ^{13}C isotopomers of ethylbenzene. Experimental spectra are shown in Figures 6 and 7. First the spectra of ^{13}C enriched α and β ethylbenzene, then the natural abundance spectrum. One of the problems is that the aromatic part, due to the overlap of the spectra of four aromatic isotopomers, is a complex set of resonances around 150 Hz that cannot be resolved.

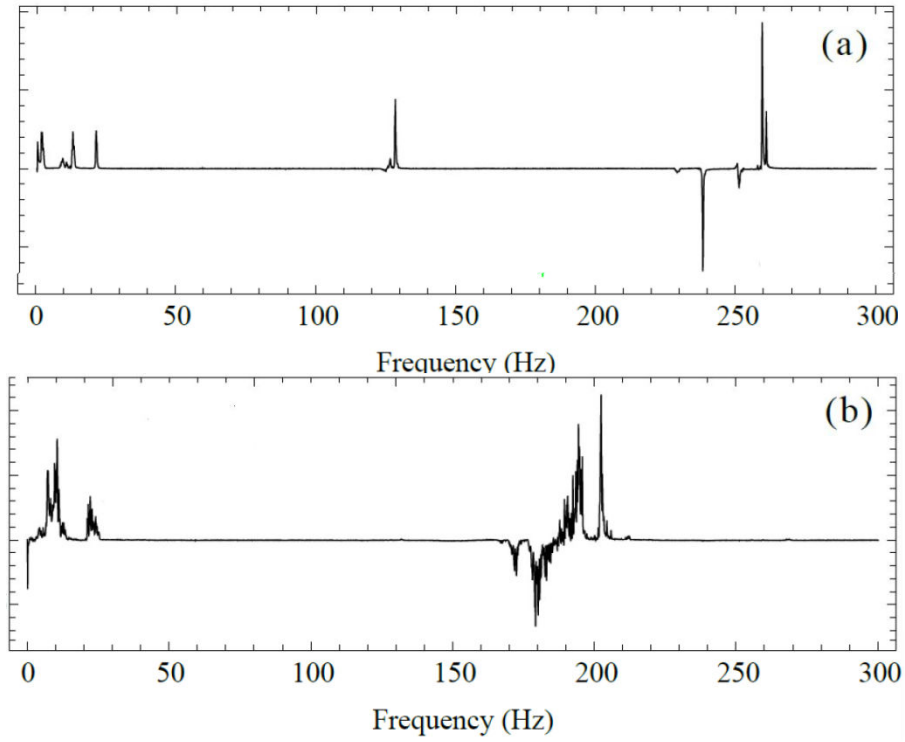

Figure 6: ZFNMR spectra (Imaginary component) of ethylbenzene-β^{13}C (a) and ethylbenzene-α^{13}C (b), polarized via addition of parahydrogen to labeled styrene. From T. Theis et al. *Nature Phys.* 2011, **7**, 571.

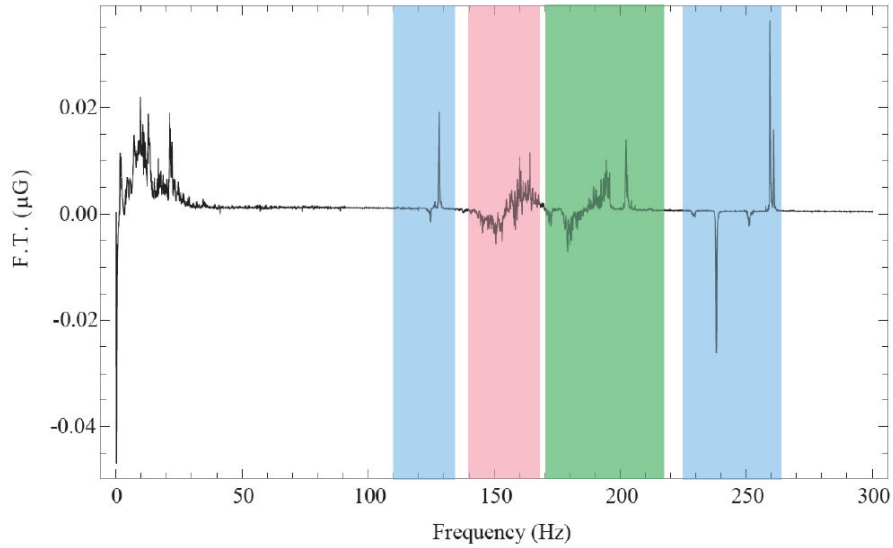

Figure 7: Zero-field J-spectrum (Imaginary component) of ethylbenzene produced, produced via parahydrogenation of styrene with ^{13}C in natural abundance. Contributions from the α and β isotopomers are easily recognizable from the spectra shown in Figure 6. The signal in the neighbourhood of 156 Hz is due to isotopomers with ^{13}C on the benzene ring. From T. Theis et al. *Nature Phys.* 2011, **7**, 571.

The calculated spin-spin coupling constants for all six isotopomers are shown in Table. The computational protocol consists in an optimization of ethylbenzene (one conformer) at the MP2/aug-cc-pVTZ level of theory followed by DFT calculations of spin-spin couplings at the BHandH/pcJ-2 level of theory.

Table 3: Calculated spin-spin couplings of ethylbenzene

	β C13	α C13	ipso C13	ortho C13	meta C13	para C13
J(*C*,C*H*$_3$)	126.54	-4.13	5.15	-0.17	0.02	0.03
J(*C*,C*H*$_2$)	-4.87	126.40	-5.75	6.42	0.02	0.57

J(*C*,H_o)	-1.25	4.87	-0.18	157.00	0.45	8.23
J(C,H_m)	0.68	0.22	8.14	0.59	159.86	0.47
J(*C*,H_p)	-1.13	0.75	-2.06	8.51	0.71	160.59
J(*C*,$H_{o'}$)	-1.25	4.87	-0.18	7.17	-1.69	8.23
J(C,$H_{m'}$)	0.68	0.22	8.14	-2.01	8.54	0.47
J(CH_3,CH_2)	8.21	8.21	8.21	8.21	8.21	8.21
J(CH_3,H_o)	-0.02	-0.02	-0.02	-0.02	-0.02	-0.02
J(CH_3,H_m)	0.00	0.00	0.00	0.00	0.00	0.00
J(CH_3,H_p)	-0.04	-0.04	-0.04	-0.04	-0.04	-0.04
J(CH_2,H_o)	-0.56	-0.56	-0.56	-0.56	-0.56	-0.56
J(CH_2,H_m)	0.37	0.37	0.37	0.37	0.37	0.37
J(CH_2,H_p)	-0.45	-0.45	-0.45	-0.45	-0.45	-0.45
J(H_o,H_m)	8.77	8.77	8.77	8.77	8.77	8.77
J(H_o,H_p)	0.65	0.65	0.65	0.65	0.65	0.65
J(H_o,$H_{m'}$)	1.07	1.07	1.07	1.07	1.07	1.07
J(H_o,$H_{o'}$)	1.36	1.36	1.36	1.36	1.36	1.36
J(H_m,H_p)	8.61	8.61	8.61	8.61	8.61	8.61
J(H_m,$H_{m'}$)	0.79	0.79	0.79	0.79	0.79	0.79
J(H_m,$H_{o'}$)	1.07	1.07	1.07	1.07	1.07	1.07

We then proceeded to the simulation of the ZFNMR spectrum for each of the six isotopomers. These are reported in the following Figures.

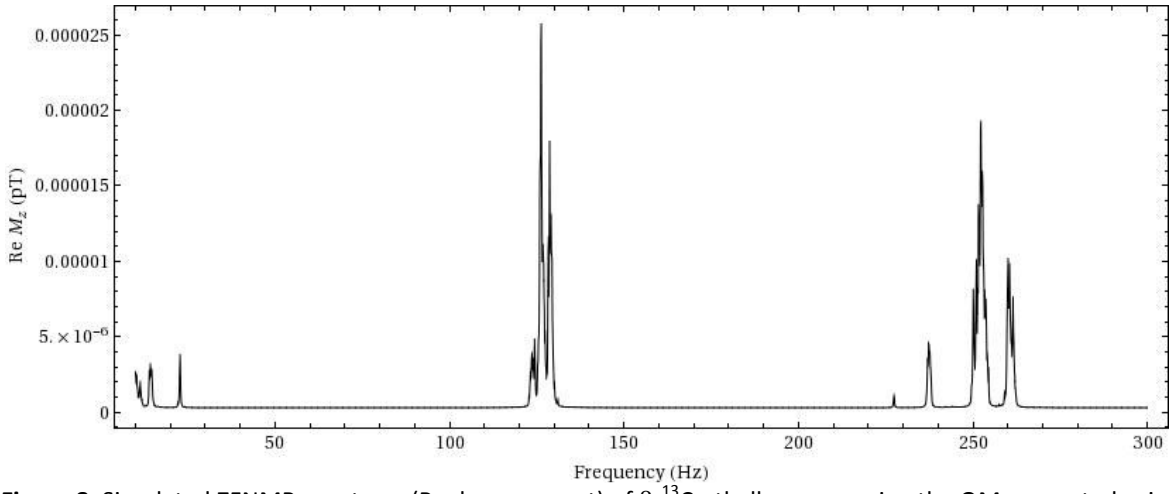

Figure 8: Simulated ZFNMR spectrum (Real component) of β-^{13}C-ethylbenzene using the QM computed spin-spin couplings

The spectrum of β-^{13}C-ethylbenzene shows the expected two main resonances at about *J* and 2*J* where *J* is the ^{1}*J*(C,H) of the methyl group. However the structure is significantly complicated by the presence of the long range couplings. Similarly, the spectrum of α-^{13}C-ethylbenzene is rather complex due to long-range couplings, though the identification of its key feature around 3/2*J* is relatively easy.

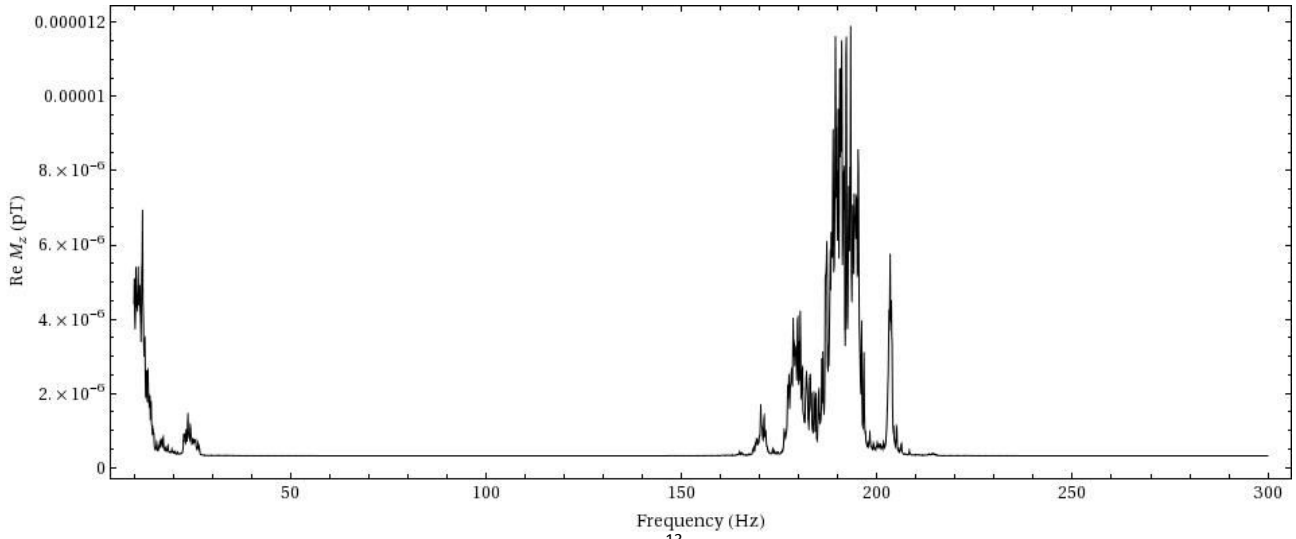

Figure 9: Simulated ZFNMR spectrum (Real component) of α-^{13}C-ethylbenzene using the QM computed spin-spin couplings

The aromatic part was the most difficult to interpret since the spectra of the four different isotopomers are overlapped in the experimental spectrum and almost impossible to disentangle.

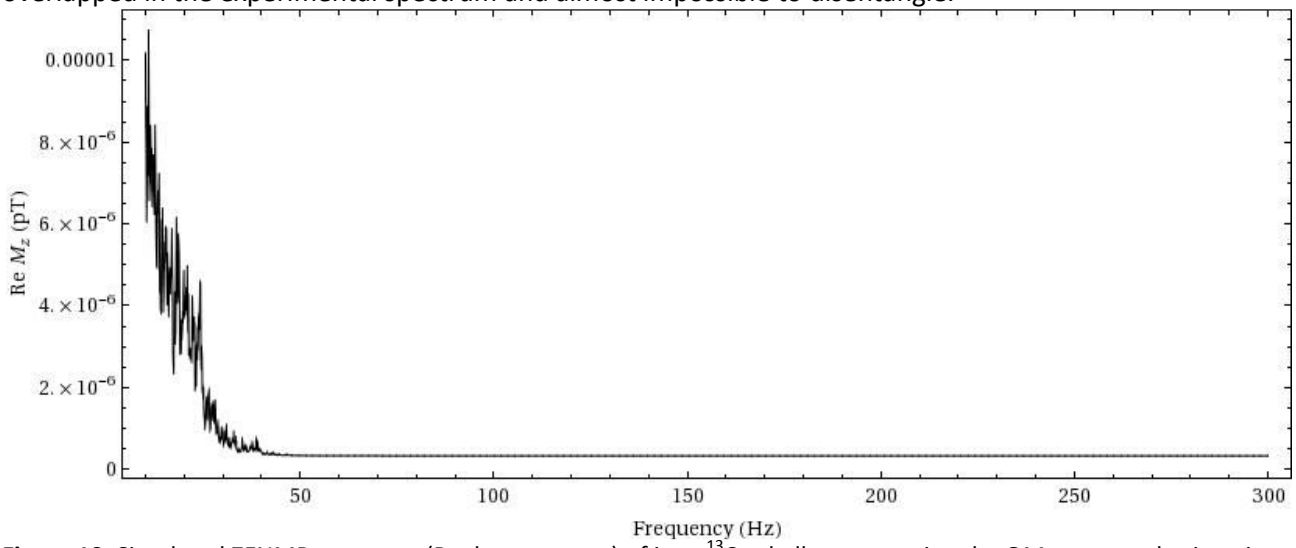

Figure 10: Simulated ZFNMR spectrum (Real component) of ipso-^{13}C-ethylbenzene using the QM computed spin-spin couplings

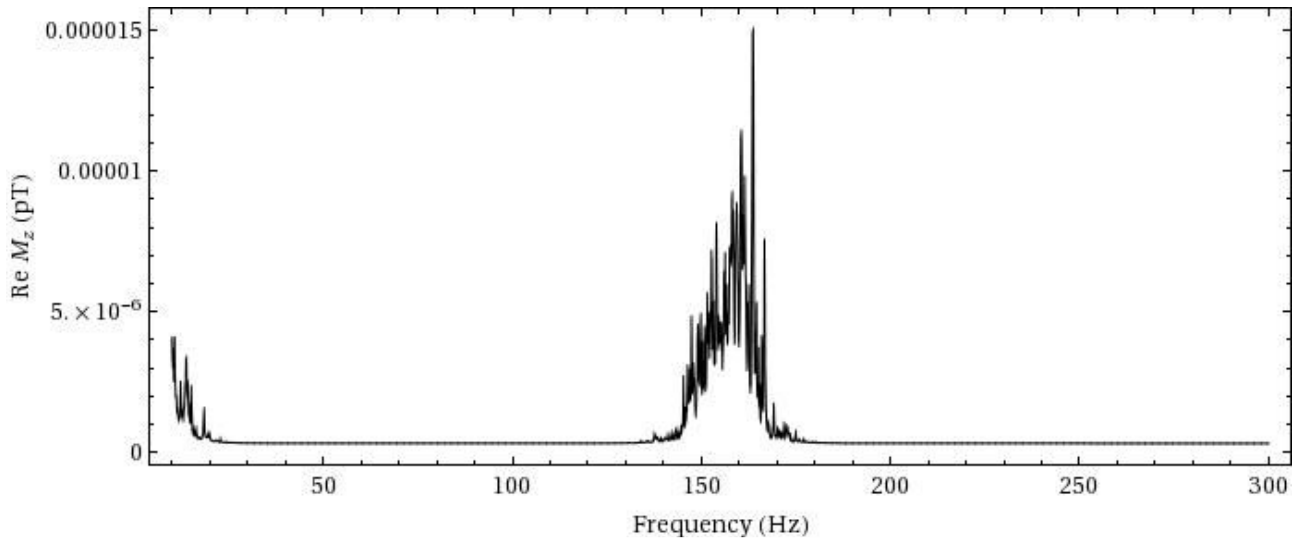

Figure 11: Simulated ZFNMR spectrum (Real component) of ortho-^{13}C-ethylbenzene using the QM computed spin-spin couplings

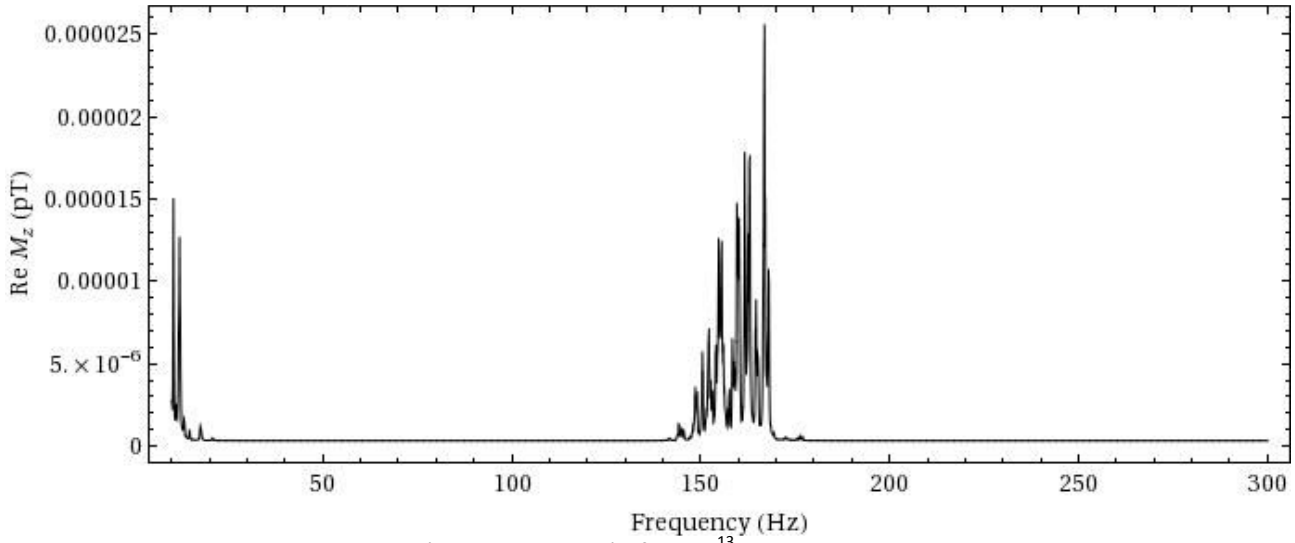

Figure 12: Simulated ZFNMR spectrum (Real component) of meta-^{13}C-ethylbenzene using the QM computed spin-spin couplings

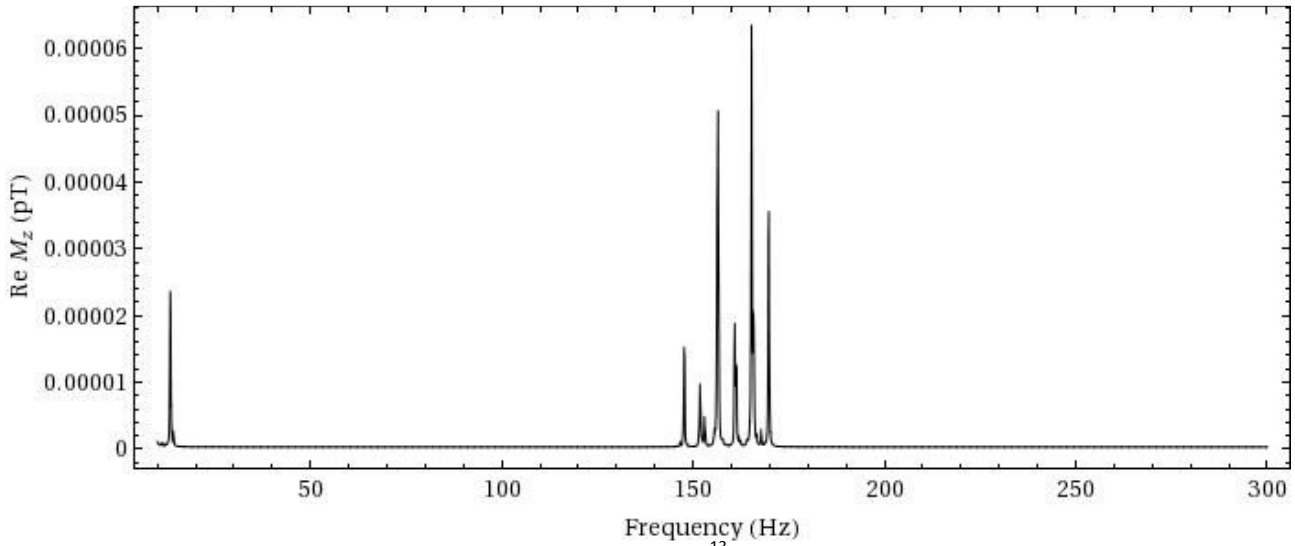

Figure 13: Simulated ZFNMR spectrum (Real component) of para-^{13}C-ethylbenzene using the QM computed spin-spin couplings

The acquisition of ZFNMR experimental spectra of EB with high signal-to-noise ratio and high resolution is currently on the way at the Berkeley's labs and a comparison and full assignment will be the subject of our future cooperative work.

Ethylene glycol (EG). The group at Berkeley had just finished a set of measurements of ZFNMR spectra of pure EG doubly labeled with ^{13}C as a function of temperature and in mixture with water (Y. Shimizu, MP Ledbetter, J Blanchard, S Pustelny, D Budker, A Pines, manuscript in preparation). The spectrum is characterized by a complex set of resonances: a strong line around 210 Hz is mainly due to the one-bond ^1J(CH) coupling since for a simple CH_2 group this is expected at 3/2J. Several other lines are present in the range 180-240 Hz plus an additional multiplet around 20 Hz, which is mainly due to the one bond ^1J(CC). For the purpose of the ZF simulation the system is, in principle, a 8-spins system: two ^{13}C, four alkyl protons and two hydroxyl protons. It is, however, unclear whether the couplings with the hydroxyl protons will affect the spectra because proton exchange is expected to take place and to be fast compared to the coupling itself. As a remarkable feature of the spectra a shift of the central resonance from 208.65±0.1 Hz at 40 °C to 208.90±0.05 at 100 °C is observed. Such a dependence on temperature can be ascribed to the

varying population of conformers of EG. Since each conformer is expected to be characterized by a different set of couplings (^1J(CH), ^1J(CC), ^2J(CH), ^3J(HH) plus the couplings with the hydroxyls) a different average will result at different temperatures based on the Boltzmann population.
For EG, 27 different conformers can be conceived, three for each dihedral angle: HOCC, OCCO and CCOH. Of these, however, only ten are independent and they are listed in Table 4. The meaning of the labels is the following: lower case g, t, g' indicates a ≈ +60°, ≈ 180° and ≈ –60° for the HOCC or CCOH dihedral angles while upper case G, T indicates gauche or trans arrangement of the OCCO dihedral angle. In Figure 14, the g'Gt conformer is shown as an example.

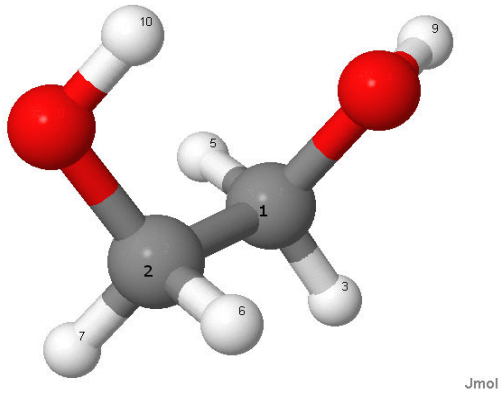

Figure 14: g'Gt conformer of ethylene glycol.

We used the following protocol for the calculation of the spin-spin coupling constants. Each conformer was optimized at the MP2/aug-cc-pVTZ level including the solvent response through the PCM model (ε = 37.7 as for pure EG). Vibrational correction to the enthalpy and entropy were evaluated at the same level of theory in order to obtain the free energy term. Then, for each optimized structure we have calculated the spin-spin coupling constants at the Density Functional Theory level, using the BHandH functional and the basis set pcJ-2. This protocol gave very good results concerning the prediction of spin-spin couplings in small organic molecules (T. Kupka et al. *J. Phys. Chem. A* **2012**, 116, 3738).

Table 4: Calculated spin-spin coupling constants for the ten conformers of EG

	g'Gg'	gGg'	gGg	gTg'	gTg	tGg'	tGg	tGt	tTg	tTt
^{1}JCH	140.80	141.74	139.97	141.94	141.93	142.01	140.30	140.57	142.13	142.24
^{1}JCC	39.88	38.08	38.60	41.15	41.15	39.73	40.82	42.95	43.54	45.95
^{2}JCH	-1.07	-1.28	-0.82	-3.82	-3.81	-2.01	-1.70	-2.58	-4.57	-5.26
^{3}JHH	4.73	4.97	4.73	9.38	9.33	4.81	4.56	4.42	9.30	9.22
^{3}JHOH	8.58	7.58	8.04	8.61	8.63	4.00	4.59	1.05	4.98	1.24
^{4}JHOH	-0.55	-0.50	-0.51	-0.14	-0.14	0.30	0.39	1.18	-0.30	-0.34
JOHOH	-0.07	0.10	-0.04	0.01	0.01	0.17	-0.02	-0.07	-0.20	0.53
^{3}JCOH	-0.67	0.98	0.06	-0.88	-0.78	5.00	4.37	8.61	5.63	12.17
^{2}JCOH	-3.45	-3.47	-3.33	-3.34	-3.43	-3.25	-3.16	-2.83	-3.11	-2.67
ΔG	0.30	0.20	1.12	1.59	1.62	0.00	1.09	1.06	1.64	1.60
N fold	2	4	2	2	2	4	4	2	4	1
Pop	0.118	0.265	0.042	0.023	0.022	0.343	0.087	0.045	0.044	0.011

Spin-spin coupling constants, after been averaged for equivalence, are listed in Table 4 for all ten independent conformers of EG. The relative free energy, ΔG, obtained from the calculations is also reported (such term includes long range solvent effects and vibrational corrections to enthalpy and entropy at 298 K). The next line reports the degeneracy of each conformer and the last entry the Boltzmann population at 298 K. Then we can calculate the average coupling at two different temperatures, here 300 K and 400 K. Though the enthalpy and entropy corrections were evaluated at 298 K this is expected to have a negligible influence on the final results. The results are reported in Table 5.

Table 5. Boltzmann averaged couplings at 300 K and 400 K.

	T = 300 K	T = 400 K
^{1}JCH	141.56	141.50
^{1}JCC	39.60	39.80
^{2}JCH	-1.79	-1.89
^{3}JHH	5.09	5.25
^{3}JHOH	5.78	5.80
^{4}JHOH	-0.05	-0.05
^{5}JOHOH	0.08	0.07
^{3}JCOH	2.99	3.01
^{2}JCOH	-3.31	-3.30

First we note that ^{2}J and ^{3}J couplings involving the hydroxyl protons are significant. Thus we have first considered a simulation of the ZFNMR spectrum at room temperature including all couplings. The results of the simulation are reported in Figure 15.

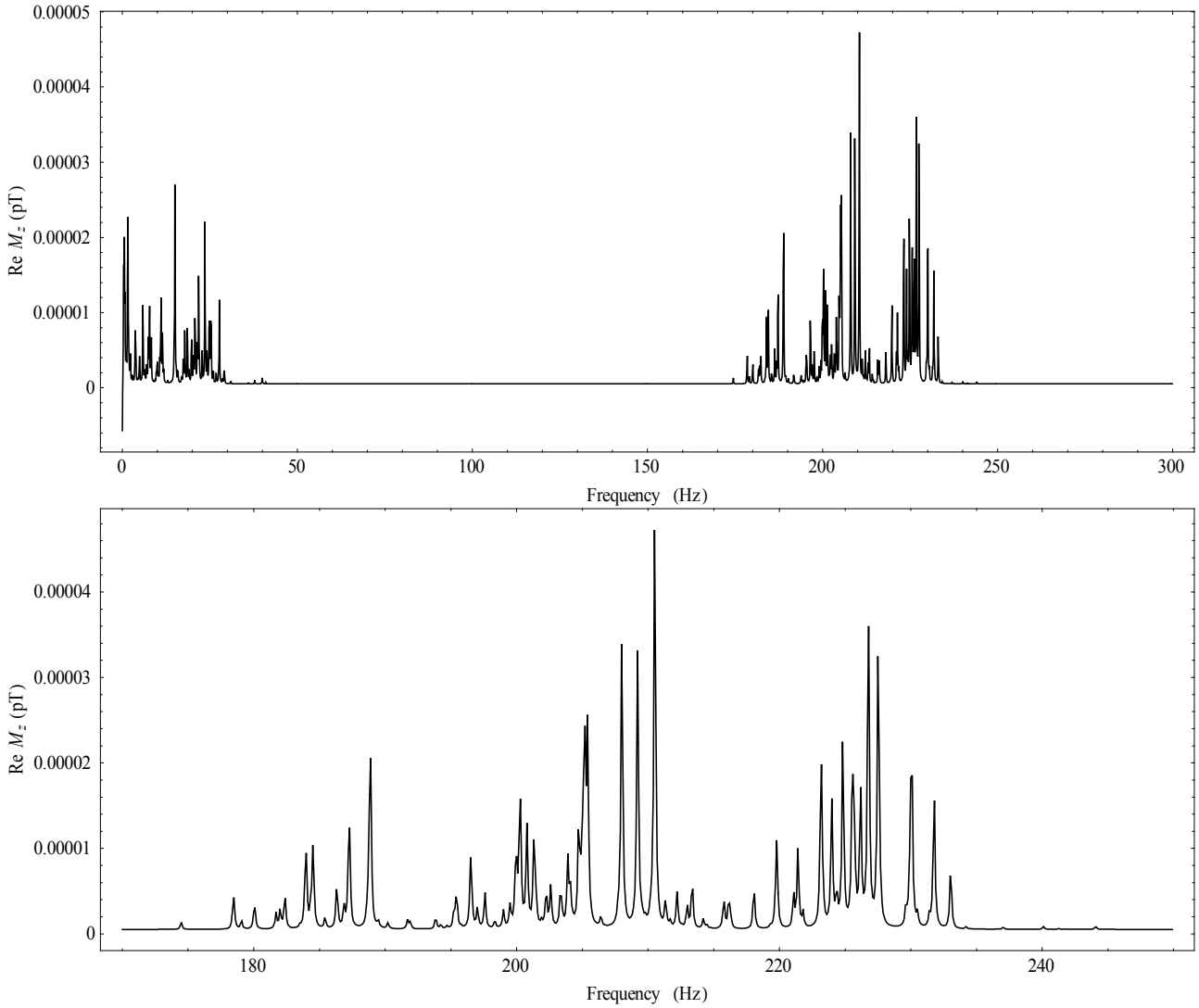

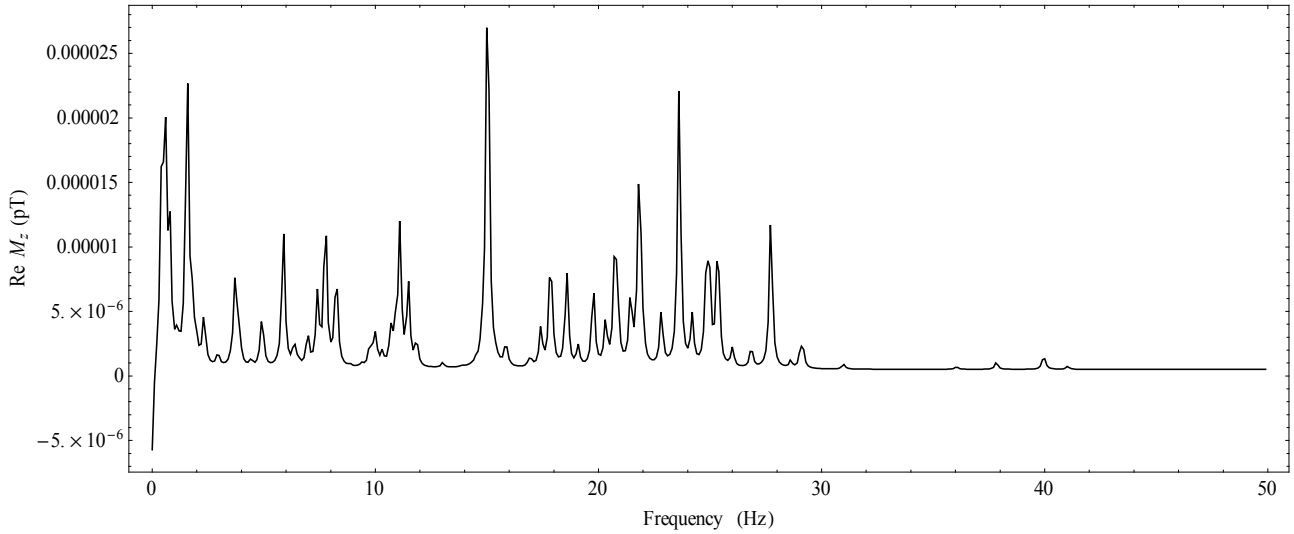

Figure 15. ZFNMR spectrum of EG simulated at 300 K including the coupling constants with the OH couplings. Top: total spectrum, middle and bottom: enlarged regions.

The simulated spectrum has no resemblance with the experimental one. This suggests that coupling with the hydroxyls does not affect the ZFNMR spectrum likely because of fast exchange of protons.
Then we have simulated the spectrum setting all couplings with the OH protons to zero. The results are shown in Figure 16 for T = 300 K. The spectrum is in very good agreement with the experiment. All the features are nicely reproduced by the simulation.

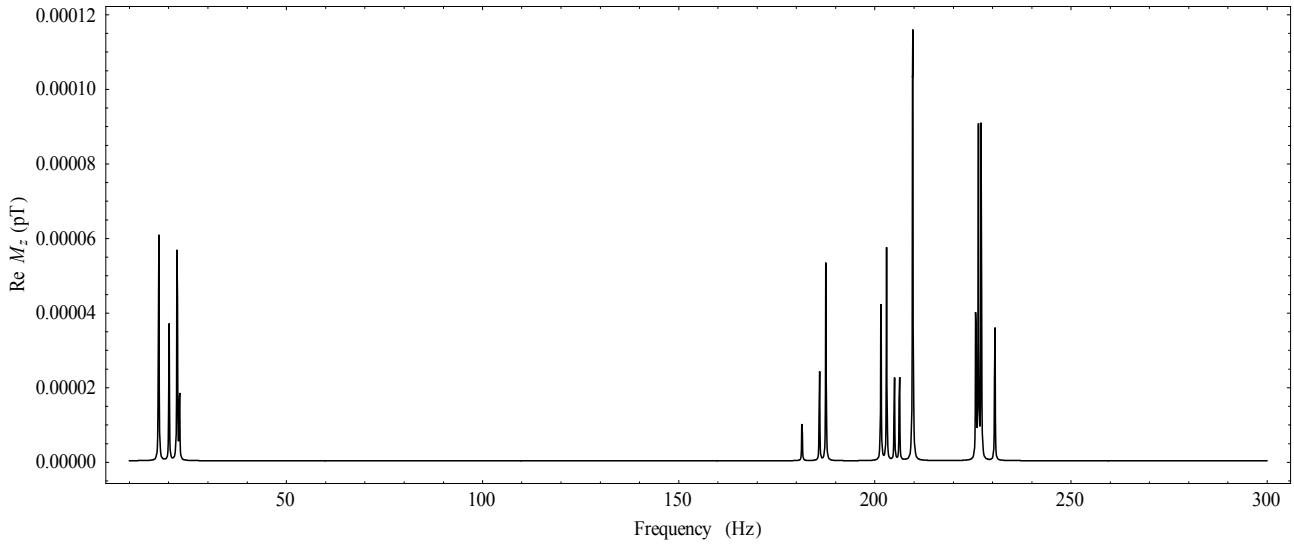

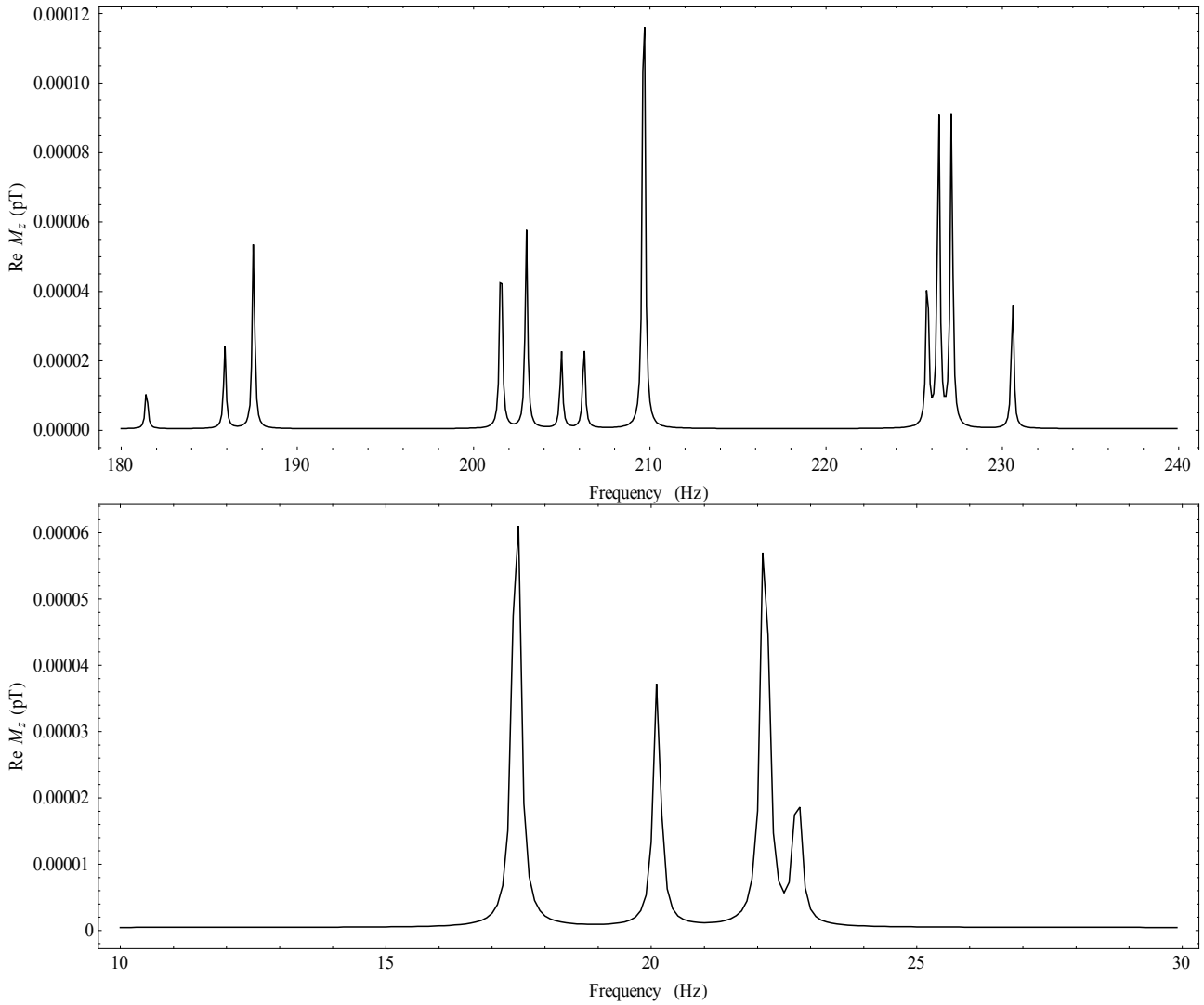

Figure 16. ZFNMR spectrum of EG simulated at 300 K without the coupling constants with the OH protons. Top: total spectrum, middle and bottom: enlarged regions. Central resonance due to ^1J(CH): 209.7 Hz

Such an agreement also suggests that the coupling with the hydroxyl protons is averaged to zero by fast proton exchange. The calculated central resonance mostly dependent on the ^1J(CH) is found at 209.7 Hz, about one Hz offset with respect to the experimental spectrum. However, given the large window of resonances (0 – 240 Hz) found this appears as a systematic error due to the calculation of the spin-spin coupling constants. Nevertheless, the variation of ^1J(CH), as well as the other couplings, with the EG conformation, see Table 4, is significant: it varies from 139.97 Hz for the *gGg* conformer up to 142.24 for the *tTt* conformer. The most stable (therefore the most populated) conformers, however, that is *tGg'* and *gGg'*, that make up to about 70% of the total population, have a rather large value of the coupling. Therefore it is expected that increasing the temperature, that is weighting more the other conformation and less the *tGg'* and *gGg'*, will lower the average coupling. This is indeed what happens, see Table 5. It is not surprising, then, that the simulated ZFNMR spectrum at 400 K, see Figure 17, shows a shift of the central resonance around 210 Hz of −0.3 Hz, that is in the opposite direction compared to the experiments.

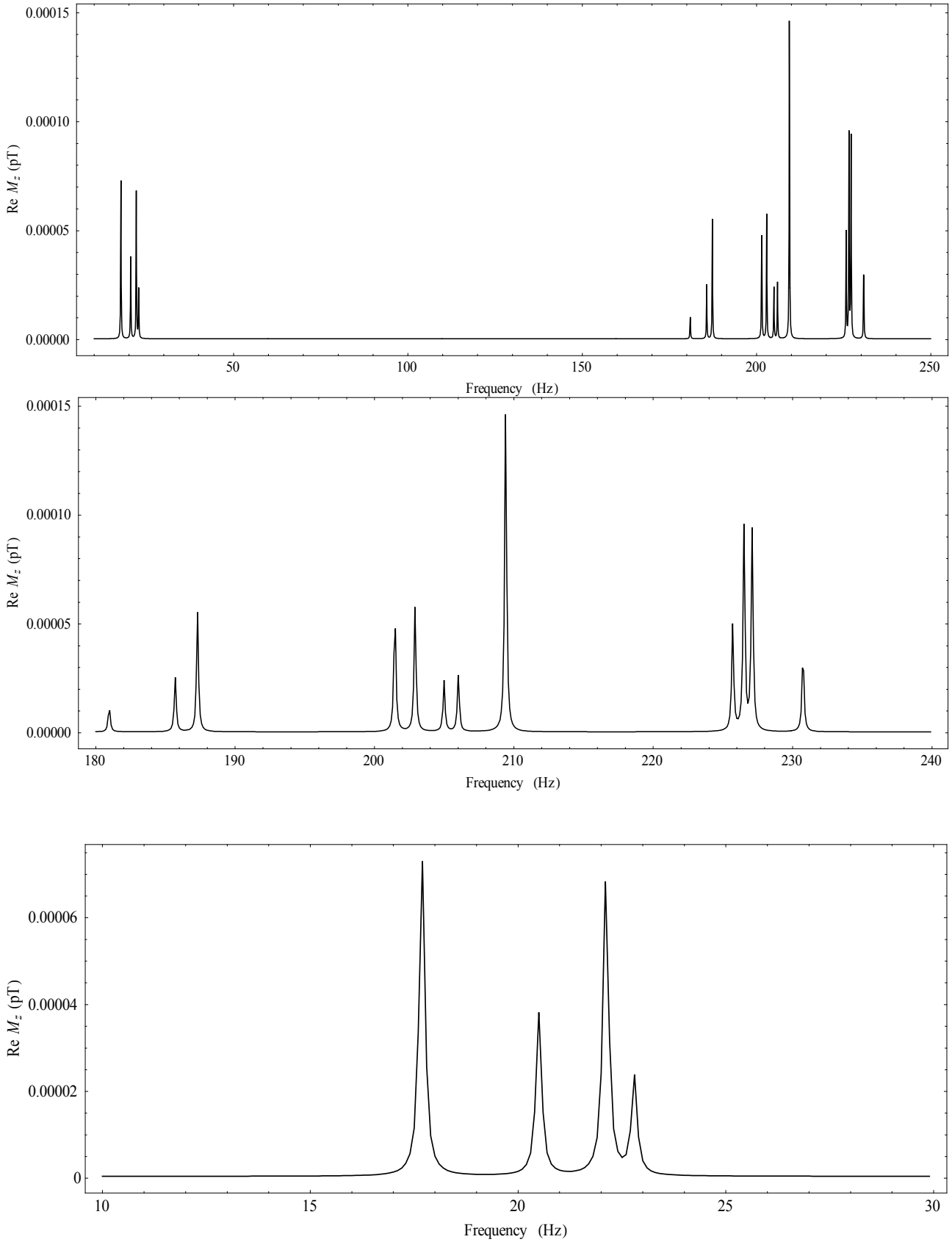

Figure 17. ZFNMR spectrum of EG simulated at 400 K without the coupling constants with the OH protons. Top: total spectrum, middle and bottom: enlarged regions. Central resonance due to ^{1}J(CH): 209.4 Hz

The conformer distribution has been evaluated for the single molecule, and, although the long range solvent effect has been included, no explicit intermolecular interactions, most importantly hydrogen bonds, have been taken into account. It is expected that the conformer distribution in solution will be strongly affected by intermolecular hydrogen bonds.
Therefore we have envisaged, together with the Berkeley group, two possible ways to obtain a detailed description of the conformer distribution in the bulk phase: a classical MD simulation with a tailored FF or a Car-Parrinello MD simulation. Such investigations, which are expected to require several months of work, will be pursued starting from the end of 2013, in close collaboration with the Berkeley group.

Conclusion

During the three weeks in Berkeley I had the possibility to start many different research activities, within the general research line presented in the STM project, in cooperation with the group of proff. Pines and Budker. These activities are now continuing, together with prof. A Bagno at the Department of Chemical Sciences of the University of Padova. The visit to the Berkeley's laboratories has indeed placed our collaborative efforts on a firmer basis and has provided the necessary stimuli to achieve the desired results.

Padova, September 5, 2013 Giacomo Saielli